Original Research

Spatial Variation in Cartilage T2 of the Knee

Harvey E. Smith, AB,[1] Timothy J. Mosher, MD,[1]* Bernard J. Dardzinski, PhD,[3,4] Belinda G. Collins, MD, PhD,[1] Christopher M. Collins, PhD,[1] Qing X. Yang, PhD,[1] Vincent J. Schmithorst, PhD,[3] and Michael B. Smith, PhD[1,2]

Technical limitations imposed by resolution and B1 homogeneity have thus far limited quantitative in vivo T2 mapping of cartilage to the patella. The purpose of this study is to develop T2 mapping of the femoral/tibial joint and assess regional variability of cartilage T2 in the knee. Quantitative in vivo T2 mapping of the knee was performed on 15 asymptomatic adults (age, 22–44) using a 3T MR scanner. There is a consistent pattern of spatial variation in cartilage T2 with longer values near the articular surface. The greatest variation occurs in the patella, where T2 increases from 45.3 ± 2.5 msec at a normalized distance of 0.33–67 ± 5.5 msec at a distance of 1.0. These results demonstrate feasibility of performing in vivo T2 mapping of femoral tibial cartilage. Except for the superficial 15% where T2 values are lower, the spatial variation in T2 of femoral and tibial cartilage is similar to patellar cartilage. J. Magn. Reson. Imaging 2001;14: 50–55. © 2001 Wiley-Liss, Inc.

Index terms: cartilage; arthritis; T2; MRI; high-field MRI

THE SYNDROME OF OSTEOARTHRITIS (OA) is a multifactorial process characterized by changes in structure and function of the joint (1). The central component of OA is degradation and subsequent loss of articular cartilage. There is currently no definitive test for OA, and the majority of patients are diagnosed after significant progression of the disease on the basis of clinical and radiographic findings. Development and application of treatment options is limited by an inability to detect and monitor preclinical cartilage damage. Because OA is strongly influenced by biomechanical factors, an understanding of biochemical and structural properties of cartilage in the intact in vivo joint is essential to understanding the pathophysiology of OA and other rheumatic diseases. A better understanding and more reliable measure of early cartilage damage would have widespread application in developing chondroprotective agents and techniques, which are likely to be more efficacious when used before there has been significant destruction of the solid cartilage matrix (2). Consequently, there is great interest in identifying sensitive, noninvasive biomarkers for cartilage degeneration.

Prior studies have demonstrated spatial dependency of cartilage T2 in both isolated cartilage explants (3–6) and in vivo human patella (7,8). Preliminary studies have correlated changes in T2 with early symptomatic degeneration in patellar cartilage (8). Since there is high prevalence of OA in the femoral/tibial joint, it is advantageous to develop similar T2 mapping techniques for this joint. The cartilage of the femoral/tibial joint is thinner than patellar cartilage and poses a significant technical challenge for measurement of cartilage T2. High-field magnetic resonance imaging (MRI), with a greater signal-to-noise ratio (SNR), allows needed high-resolution T2 maps to accurately quantify the T2 profile. The femoral/tibial joint is a weight-bearing joint and is subjected to different biomechanical stresses than patellar cartilage. Quantitative T2 mapping of the entire knee may provide information about how in vivo biomechanical forces alter T2 properties of cartilage, providing information about the macromolecular organization of cartilage in different joint regions. The purposes of this project are to demonstrate the feasibility of quantitative T2 mapping of the femoral/tibial joint and to determine if spatial variation of cartilage T2 in this joint is similar to that previously observed in the patella (7,8).

MATERIALS AND METHODS

Patient Population

We performed quantitative T2 mapping of the patella and femoral/tibial joint in 15 asymptomatic male volunteers (age, 22–44; mean ± SD, 28 ± 5 years). After the nature of the procedure was explained, all participants provided informed consent to participate in the study, which was approved by the institutional review board. Immediately before the MRI examination, volun-

[1]Center for NMR Research, Department of Radiology, Pennsylvania State University College of Medicine, Milton S. Hershey Medical Center, Hershey, Pennsylvania.

[2]Department of Cellular and Molecular Physiology, Pennsylvania State University College of Medicine, Milton S. Hershey Medical Center, Hershey, Pennsylvania.

[3]Imaging Research Center, TCHRF, Children's Hospital Medical Center, Cincinnati, Ohio.

[4]Departments of Radiology and Pediatrics, University of Cincinnati College of Medicine, Cincinnati, Ohio.

Contract grant sponsor: Arthritis Foundation.

Presented at the 8th Annual Meeting of the International Society for Magnetic Resonance in Medicine, Denver, Colorado, April 1–7, 2000.

*Address reprint requests to: T.J.M., Department of Radiology/NMR Building M108, Milton S. Hershey Medical Center, 500 University Drive, Hershey, PA 17033. E-mail: tmosher@psu.edu

Received July 14, 2000; Accepted December 27, 2000.

teers completed a Western Ontario and McMaster Universities (WOMAC) OA questionnaire (9) to assess symptoms. Volunteers were classified as asymptomatic if their normalized WOMAC score was less than 10.

Image Acquisition

MR images of the patella and femoral/tibial joint were obtained with a 3.0 T MRI spectrometer (Medspec S300; Bruker Instruments, Ettlingen, Germany) with either a 14-cm-diameter saddle coil (5 patients) or a 14-cm-diameter transmit-receive linear birdcage coil (10 patients) operating at 125 MHz for protons. Image acquisitions used an asymmetric gradient insert capable of delivering ±5 G/cm of field profile. Volunteers were positioned supine within the imager, with the femoral/tibial joint placed at the gradient isocenter and the knee positioned in 5° external rotation. To optimize reproducibility in positioning, the same individual positioned each volunteer. This study did not control for potential diurnal variation in articular cartilage.

Patellar cartilage was evaluated with five axial slices with the following parameters: repetition time/echo time = 1500 msec/7.5 msec, echo train = 11, section thickness = 3 mm, field of view (FOV) = 14.0 cm, matrix = 256 × 256, bandwidth = 75.8 KHz, section selection and refocusing pulse duration = 2 msec. In-plane image resolution was 547 μm. Spin echo (SE) images were obtained through the patella in the axial plane, prescribed on the basis of a sagittal locator image. Frequency encoding was anterior to posterior to prevent pulsation artifact from the popliteal artery.

Femoral/tibial cartilage was evaluated with two sagittal slices with the following parameters: repetition time/echo time = 1500 msec/10 msec, echo train = 11, section thickness = 4 mm, FOV = 12.75 cm, matrix = 384 × 384, bandwidth = 75.8 KHz, section selection and refocusing pulse duration = 2 msec. SE images were obtained through the femoral/tibial joint in the sagittal plane, prescribed on the basis of a coronal locator image, with the slice positioned in the center of the medial and lateral femoral condyle. This location was chosen to minimize in-plane curvature of the articular cartilage that would increase volume averaging at the cartilage interfaces. Frequency encoding was head to foot across the femoral/tibial joint. Images were reconstructed to a 512 × 512 matrix, with a resulting in-plane pixel resolution of 250 μm.

Data Analysis

Magnitude images and T2 maps were calculated from 10 SE images by means of linear least-squares curve fitting on a pixel-by-pixel basis with Cincinnati Children's Hospital Image Processing Software/Interactive Data Language (CCHIPS/IDL) software (RSI, Inc., Boulder, CO) (10). Because echoes 2–11 contain a signal from the stimulated echo, exclusion of the initial SE minimizes the artifact in the T2 calculation. The influence of this error in determination of in vivo T2 measurement has been previously discussed (7,11). Fitting of the signal intensity (SI) for the *ith*, *jth* pixel as a function of time, t, can be expressed as follows:

$$SI_{i,j}(t) = SIO_{i,j} \cdot \exp(-t/T2_{i,j}),$$

where $SI0_{i,j}$ is the pixel intensity at t = 0 and $T2_{i,j}$ is the T2 time constant of pixel *i,j*. A magnitude image is generated from the pixel $SI0_{i,j}$ data, and a T2 map is generated from the $T2_{i,j}$ data.

To define regions of interest (ROI), segmentation of the articular cartilage was performed on each section of the T_2 maps using an interactive subroutine in the CCHIPS/IDL software. For the entire ROI, the software automatically generates multiple T_2 profiles by defining perpendicular tangents to the subchondral bone interface. For comparison between volunteers, each profile was normalized for cartilage thickness such that cartilage at the subchondral surface has a normalized distance of 0.0 and cartilage at the articular surface has a normalized distance of 1.0.

Analysis of T2 Profiles

A comparison of response functions was used to assess the spatial variation of T2 with respect to distance from the subchondral surface. The response function is a mathematical equation that best approximates T2 as a function of normalized distance for the population. To minimize bias in selection of a response function, profiles from all three regions (patella, femur, and tibia) were pooled and fit to 3665 candidate equations with a standard commercially available curve-fitting software package (Tablecurve; Jandel Scientific Software, San Rafael, CA). The response function was determined by sorting the fit of candidate equations by a degree of freedom adjusted r^2. Because data consistently demonstrated a best fit to polynomial equations, singular value decomposition was used in the fitting process to minimize error when fitting to higher-order polynomials. Data from the birdcage and saddle coils were initially analyzed separately to ensure that there was no difference due to the type of coil. Data from the two coils were then pooled. The medial and lateral sagittal slices from the femur and tibia were also analyzed separately to ensure that there was no significant difference between locations. After determining that there was no difference between medial and lateral slices for both the tibia and femur, data were pooled for these two regions.

The response function used to approximate the spatial variation in T2 of the normalized profiles of the entire data set was $T2 = a + bx + cx^2 + dx^3 + ee^x$. The data were then stratified by location, and this function was fit to pooled T2 profiles from patellar, femoral, and tibial cartilage. The 99.99% CI for the response function of each region was calculated to determine the difference in T2 between regions as a function of normalized distance. Regions of the response function where there was no overlap of the 99.99% CI were considered significantly different, with a Bonferroni-corrected *P* value less than 0.05.

Prior studies have indicated possible orientation dependence to T2 values of the radial zone of cartilage due to the high degree of tissue anisotropy (4,12). Due to curvature of the femoral condyle, orientation of collagen fibers in femoral cartilage may produce variation in cartilage T2 that may confound interpretation of re-

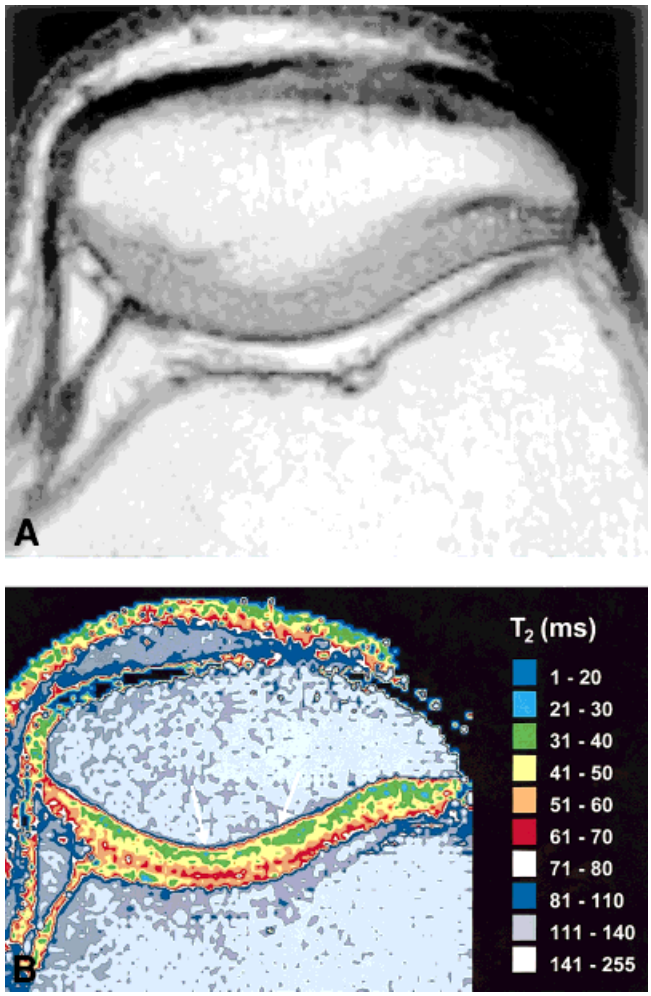

Figure 1. Calculated magnitude image (**A**) and color map of T2 (**B**) in patellar cartilage from an asymptomatic young adult male. The T2 map demonstrates a thin lamina of high T2 at the cartilage/bone interface (arrow), followed by low T2 values that increase progressively from the radial to the superficial zone.

sults. For regional comparisons in this study, only the uncovered weight-bearing cartilage of the femoral/tibial joint was profiled. This region was defined as the articulating cartilage located between the posterior edge of the anterior meniscal horn and the anterior edge of the posterior meniscal horn. This corresponds to cartilage oriented parallel to B_0.

RESULTS

Figures 1 and 2 depict the calculated magnitude and color-coded T2 images from representative data sets. Response functions from the patella, femur, and tibia from asymptomatic individuals are presented in Figure 3. All areas demonstrate a similar pattern of spatial variation in cartilage T2 with longer values observed near the articular surface. The greatest variation in cartilage T2 is in the patella, where T2 increases from 45.3 ± 2.5 msec at a normalized distance of 0.33 to 67.0 ± 5.5 msec at a distance of 1.0. There is less variation in the femoral and tibial cartilage where T2 increases from 46.0 ± 3.4 msec at a normalized distance of 0.36 to 55.7 ± 7.7 msec at a normalized distance of 1.0, and 45.5 ± 3.9 msec at a normalized distance of 0.38 to 55.0 ± 8.7 msec at a normalized distance of 1.0, respectively (mean ± 99.99% CI). As shown in Figure 4, the cartilage T2 profile for the tibia was significantly different from that of the patella from a normalized distance of 0.84–1.0. The femur T2 profile was significantly different from the patella over a normalized distance of 0.95–1.0.

DISCUSSION

The shape of the patellar T2 profile presented in Figure 3 differs from that reported in prior work by Mosher et al. (8) and Dardzinski et al. (7), which examined patellar cartilage at 3T with a surface coil. Their prior work demonstrated a monotonic increase in T2, reaching a maximum of 67 ± 2 msec in the outer transitional/superficial zone. The range of our patellar T2 profile is consistent with prior in vivo data, as well as with values observed in studies with ex vivo cartilage plugs (3,6). However, the shape of the T2 profile differs from prior in vivo reports (7,8). It decreases from a maximum of 74.1 ± 5.4 msec at a normalized distance of 0 to a minimum of 45.3 ± 2.5 msec at a normalized distance of 0.33, and then increases monotonically to the articular surface. This study used an automated segmentation routine, allowing the computer to determine the best boundary for the cartilage/bone interface. Prior work by Mosher et al. (8) and Dardzinski et al. (7) used a manual segmentation routine and was by its nature more conservative in determining the cartilage/bone interface. Using the automated segmentation routine of CCHIPS/IDL provides a reproducible method of analysis that reduces observer bias in determining cartilage boundaries. However, extending the ROI closer to the bone introduces an artifact due to volume averaging of cartilage with the bone in voxels composing the interface. This is most problematic at the bone/cartilage interface, where chemical shift misregistration from fatty marrow will contaminate the T2 measurement of the radial zone of articular cartilage. With acquisition parameters employed in this protocol, the chemical shift misregistration is approximately 2.3 pixels for femoral cartilage and 1.5 pixels for patellar cartilage. It is likely that the longer T2 values observed over the normalized distance of 0.0–0.3 are a result of volume averaging and chemical shift misregistration artifact.

The thin femoral/tibial articular cartilage poses unique technical challenges not encountered with T2 mapping of patellar cartilage. First, femoral/tibial articular cartilage is approximately 2.5 mm thick, compared to 4.5 mm for patellar cartilage. To accurately resolve underlying spatial variation in cartilage T2 and minimize volume averaging at the cartilage interfaces, high-resolution T2 maps must be obtained. In our protocol, T2 maps of the femoral/tibial cartilage were acquired at a pixel resolution of 332 μm, compared to 547 μm for patellar cartilage. At this resolution each pixel corresponds to a normalized distance

of 0.13 in the femoral/tibial T2 profiles and 0.12 in patellar T2 profiles. Second, because of the short T2 of cartilage, short interecho times are necessary to accurately characterize the T2 decay curve. This protocol used an interecho time of 10 msec for femoral/tibial T2 maps and 7.5 msec for patellar T2 maps. The use of high matrices in the read direction for femoral/tibial T2 mapping, in combination with short interecho times, requires high receiver bandwidth to minimize data acquisition time, in this case, 75.8 KHz. A

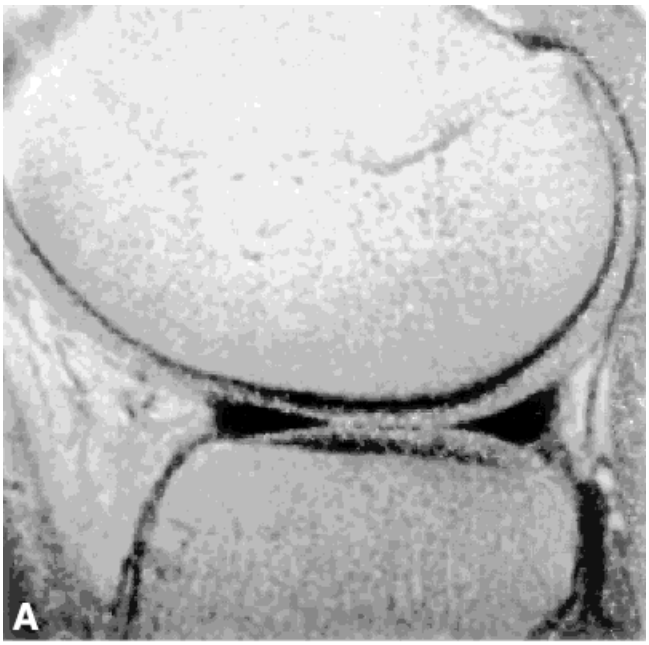

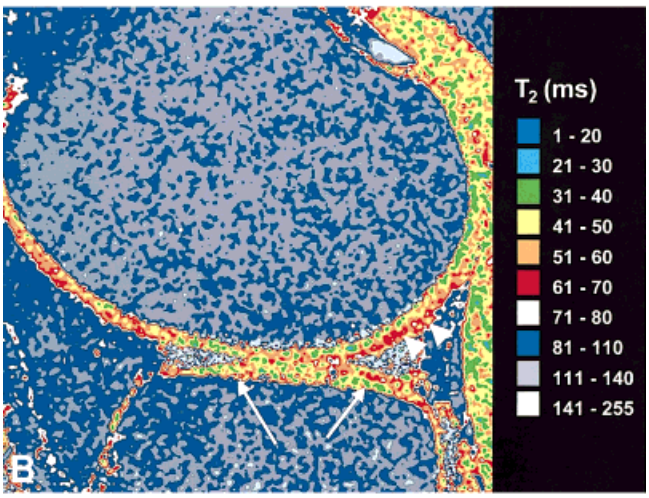

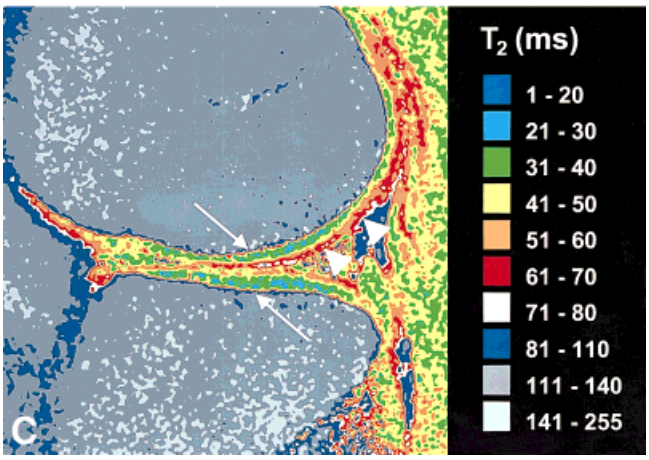

Figure 2. Calculated magnitude image (**A**) and color map of T2 (**B**) in the femoral/tibial joint from an asymptomatic young adult male. The T2 map demonstrates a laminar appearance to the T2 zones, similar to that seen in patella. As illustrated in the T2 map from a different volunteer (**C**), the T2 increases progressively from the radial to the superficial zone. Note the longer T2 in the transitional and superficial cartilage in the non-weight-bearing region of the femur (arrowhead), compared to weight-bearing cartilage.

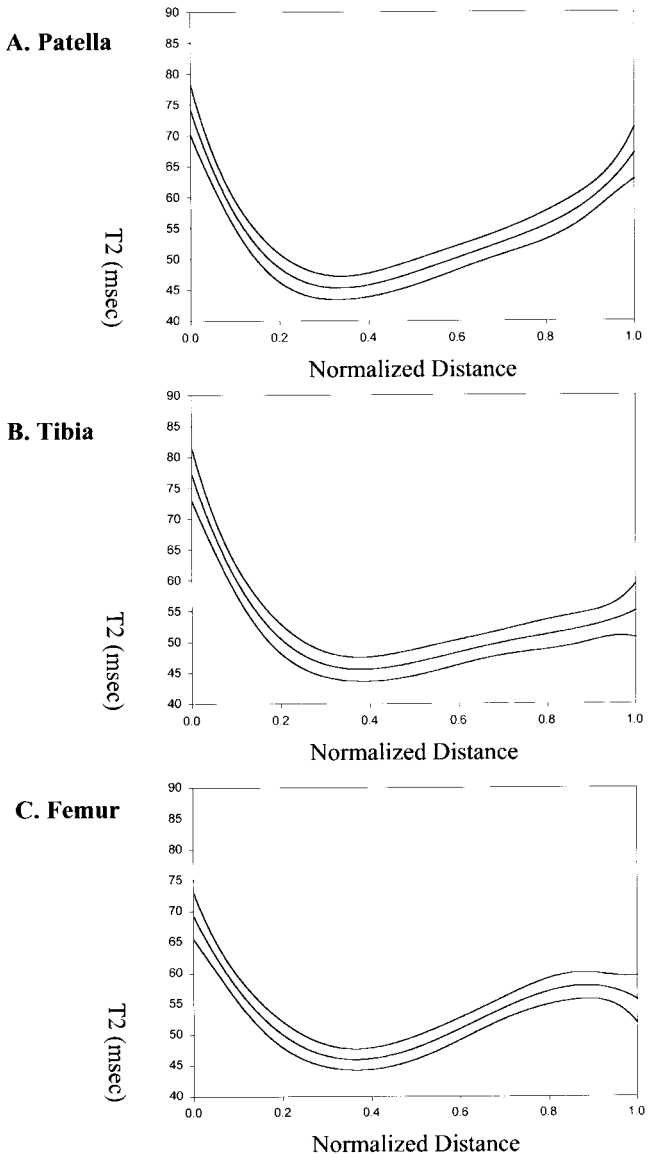

Figure 3. Spatial variation in T2 as a function of normalized distance from subchondral bone (0.0) to articular surface (1.0) (mean ± 99.99% CI) For the patella (**A**), uncovered weight-bearing tibial cartilage (**B**) and uncovered weight-bearing femoral cartilage (**C**). For all sites, cartilage T2 increases toward the articular surface; however, this increase is less in the weight-bearing cartilage of the femur and tibia.

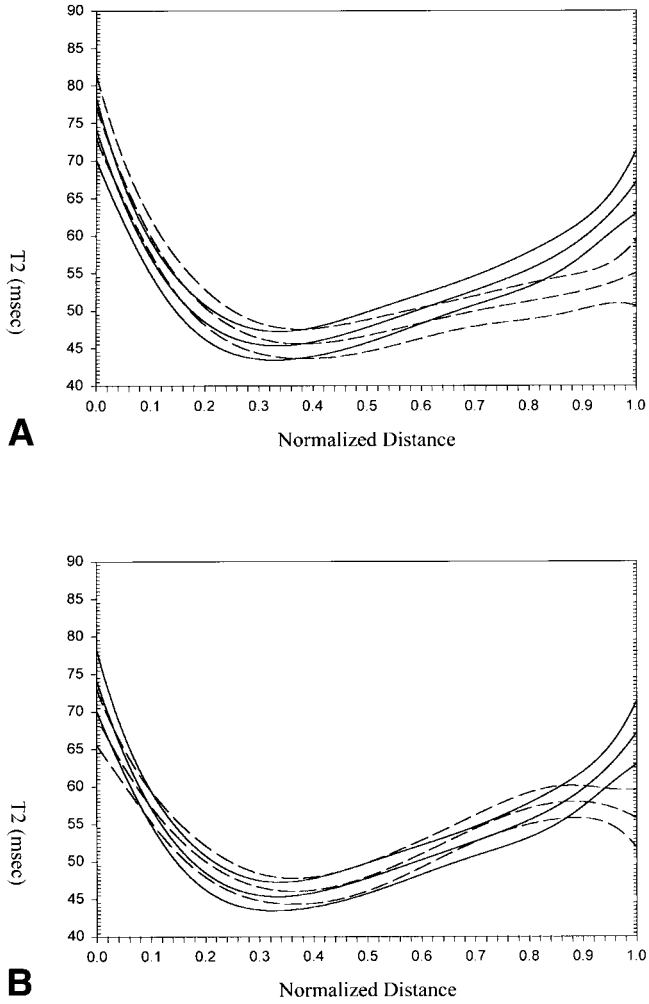

Figure 4. Comparison of patellar (solid) and tibial (dashed) T2 profiles (**A**) and patellar (solid) and femoral (dashed) T2 profiles (**B**) as a function of normalized distance from subchondral bone (0.0) to articular surface (1.0) (mean ± 99.99% CI). The patella and tibia are statistically significantly different from a normalized distance of 0.84–1.0. The patella and femur are statistically significantly different from a normalized distance of 0.95–1.0. (Bonferroni-corrected, $P < 0.05$).

dedicated gradient insert was used to obtain this bandwidth. Third, the large receiver bandwidth combined with high-resolution T2 mapping reduces the SNR. While T2 mapping of patellar cartilage has been demonstrated on clinical 1.5 T systems (13), the lower SNR may preclude T2 mapping of femoral/tibial cartilage on low-field systems.

The shape of the T2 profile for the femur and tibia is similar to that of the patella. However, both the femur and tibia have less spatial variation than the patella, with the tibia being significantly different from the patella over a normalized distance of 0.84–1.0. Known biomechanical and biochemical differences between different regions of cartilage may account for these differences. The femoral/tibial joint is weight-bearing and is under resting compression from ligament and muscle tension. Rubenstein et al. (14) demonstrated with ex vivo cartilage samples that the zonal appearance of cartilage in T2 images is dependent on the degree of compression applied to the cartilage sample, likely due to a combination of net water loss and change in collagen fiber orientation. Previous studies examining regional tissue deformation with compression have demonstrated greater compressibility of superficial cartilage (15). A possible explanation for the lower T2 of superficial femoral and tibial weight-bearing cartilage is that with compression there is preferential water loss from superficial cartilage.

In addition to biomechanical differences, there are known biochemical differences between patellar and femoral/tibial cartilage. Prior ex vivo studies indicate patellar cartilage has higher water and lower proteoglycan content than femoral cartilage (16). Additional studies are needed to determine how regional differences in cartilage composition, structure, and biomechanics influence in vivo cartilage T2 maps.

CONCLUSION

These results demonstrate for the first time the feasibility of performing quantitative in vivo T2 mapping of the entire knee. Although a similar pattern of T2 variation is observed in T2 profiles from patellar, femoral, and tibial cartilage, less spatial variation is observed in the femoral tibial joint. Resting compression of the femoral/tibial joint by muscle and ligament tension may alter both water content and solid matrix orientation, particularly in the superficial 15% of cartilage. Quantitative T2 mapping of knee articular cartilage may provide a sensitive tool for the in vivo evaluation of cartilage physiology and pathology.

ACKNOWLEDGMENTS

Harvey Smith is a Howard Hughes Medical Institute Medical Student Research Training Fellow. Timothy Mosher and Bernard Dardzinski gratefully acknowledge grant support from the Arthritis Foundation.

REFERENCES

1. Altman R. The syndrome of osteoarthritis. J Rheumatol 1997;24: 766–777.
2. Kraus VB. Pathogenesis and treatment of osteoarthritis. Med Clin North Am 1997;81:85–112.
3. Xia Y, Farquhar T, Burton-Wurster N, Ray E, Jelinski LW. Diffusion and relaxation mapping of cartilage-bone plugs and excised disks using microscopic magnetic resonance imaging. Magn Reson Med 1994;31:273–282.
4. Xia Y, Farquhar T, Burton-Wurster N, Lust G. Origin of cartilage laminae in MRI. J Magn Reson Imaging 1997;7:887–894.
5. Mlynarik V, Degrassi A, Toffanin R, Jarh O, Vittur F. A method for generating magnetic resonance microimaging T2 maps with low sensitivity to diffusion. Magn Reson Med 1996;35:423–425.
6. Mlynarik V, Degrassi A, Toffanin R, Vittur F, Cova M, Pozzi-Mucelli RS. Investigation of laminar appearance of articular cartilage by means of magnetic resonance microscopy. Magn Reson Imaging 1996;14:435–442.
7. Dardzinski BJ, Mosher TJ, Li S, Van Slyke MA, Smith MB. Spatial variation of T2 in human articular cartilage. Radiology 1997;205: 546–550.
8. Mosher TJ, Dardzinski BJ, Smith MB. Human articular cartilage: influence of aging and early symptomatic degeneration on the spatial variation of T2—preliminary findings at 3 T. Radiology 2000; 214:259–266.

9. Bellamy N, Buchanan WW, Goldsmith CH, Campbell J, Stitt LW. Validation study of WOMAC: a health status instrument for measuring clinically important patient relevant outcomes to antirheumatic drug therapy in patients with osteoarthritis of the hip or knee. J Rheumatol 1988;15:1833–1840.
10. Dardzinski B, Schmithorst V, Mosher T. Entropy mapping of articular cartilage. In: Proceedings of the 7th Annual Meeting of ISMRM, Philadelphia, 1999. p 1018.
11. Poon CS, Henkelman RM. Practical T2 quantitation for clinical applications. J Magn Reson Imaging 1992;2:541–553.
12. Rubenstein JD, Kim JK, Morova-Protzner I, Stanchev PL, Henkelman RM. Effects of collagen orientation on MR imaging characteristics of bovine articular cartilage. Radiology 1993;188: 219–226.
13. Frank LR, Wong EC, Luh WM, Ahn JM, Resnick D. Articular cartilage in the knee: mapping of the physiologic parameters at MR imaging with a local gradient coil—preliminary results. Radiology 1999;210:241–246.
14. Rubenstein JD, Kim JK, Henkelman RM. Effects of compression and recovery on bovine articular cartilage: appearance on MR images. Radiology 1996;201:843–850.
15. Guilak F, Ratcliffe A, Mow VC. Chondrocyte deformation and local tissue strain in articular cartilage: a confocal microscopy study. J Orthop Res 1995;13:410–421.
16. Froimson MI, Ratcliffe A, Gardner TR, Mow VC. Differences in patellofemoral joint cartilage material properties and their significance to the etiology of cartilage surface fibrillation. Osteoarthritis Cartilage 1997;5:377–386.